

A note on the stability of slip channel flows

Eric Lauga^{a)}

Division of Engineering and Applied Sciences, Harvard University, Cambridge, Massachusetts 02138

Carlo Cossu^{b)}

*Laboratoire d'Hydrodynamique (LadHyX), Centre National de la Recherche Scientifique (CNRS)—
École Polytechnique, Palaiseau Cedex 91128, France*

(Received 5 April 2005; accepted 7 July 2005; published online 23 August 2005)

We consider the influence of slip boundary conditions on the modal and nonmodal stability of pressure-driven channel flows. In accordance with previous results by Gersting [“Hydrodynamic stability of plane porous slip flow,” *Phys. Fluids* **17**, 2126 (1974)] but in contradiction with the recent investigation of Chu [“Instability of Navier slip flow of liquids,” *C. R. Mec.* **332**, 895 (2004)], we show that the slip increases significantly the value of the critical Reynolds number for linear instability. The nonmodal stability analysis, however, reveals that slip has a very weak influence on the maximum transient energy growth of perturbations at subcritical Reynolds numbers. Slip boundary conditions are therefore not likely to have a significant effect on the transition to turbulence in channel flows. © 2005 American Institute of Physics.

[DOI: 10.1063/1.2032267]

The advances in microfabrication techniques using polymeric or silicon-based materials has allowed us to gain a significant understanding on the behavior of fluids at small scales.^{1–3} One topic of current interest concerns the validity of the no-slip boundary condition for Newtonian liquids near solid surfaces.^{4–8} A large number of recent experiments on small scales with flow driven by pressure gradients, drainage, shear, or electric field have reported an apparent breakdown of the no-slip condition, with slip lengths possibly as large as microns. The slip length λ is defined as the ratio of the surface velocity to the surface shear rate; $\lambda=0$ corresponds to a no-slip condition, and $\lambda=\infty$ to a perfectly slipping surface.

Since the transition to turbulence in wall-bounded flows occurs at large values of the Reynolds number, studies in shear-flow instabilities have usually been outside the realm of microfluidics. However, a set of recent investigations of the linear modal stability of pressure-driven flows in two-dimensional channels^{9–11} has reported that slip boundary conditions decrease the critical Reynolds number, from $Re=5772$ (its classical no-slip value obtained for Poiseuille flow) to $Re\approx 100$, in strong disagreement with early calculations of Gersting.¹² Such results would potentially have a major impact on both turbulence and microfluidic studies.

The goal of this Brief Communication is twofold. First, we resolve the disagreement between the above cited results. A careful analysis of the derivation of the equations used in Refs. 9–11 reveals that incorrect slip boundary conditions on the perturbations were used in the modal stability analysis. The use of the appropriate boundary conditions on the perturbations reveals the strongly stabilizing effect of slip on the

eigenvalues of the linear stability operator, confirming earlier results.¹² Recent advances in the domain of shear-flow instabilities have, however, revealed the usual lack of relevance of the modal stability analysis, contrasted to the nonmodal stability analysis, in the subcritical transition in channel flows (for a review see, e.g., Refs. 13 and 14). The second goal of this Brief Communication is therefore to quantify the effect of slip on the nonmodal stability of viscous channel flows. To this end, we compute the maximum transient energy growth¹⁵ in the presence of slip at subcritical Reynolds numbers. We find that, for all the considered combinations of streamwise and spanwise wavenumbers, the effect of slip on the maximum energy growth and on the associated optimal perturbations is weak.

We consider the flow between two parallel plates located at $y^*=\pm h$ of a Newtonian fluid with viscosity μ driven by a constant pressure gradient dp^*/dx^* in the x^* direction. If we nondimensionalize lengths by h , velocities by $U_{\text{ref}}=h^2(-dp^*/dx^*)/2\mu$, time by h/U_{ref} , and pressure by ρU_{ref}^2 , the dimensionless incompressible Navier-Stokes equations for the velocity and pressure fields, (\mathbf{u}, p) , read as

$$\left(\frac{\partial}{\partial t} + \mathbf{u} \cdot \nabla\right)\mathbf{u} = -\nabla p + \frac{1}{\text{Re}}\nabla^2\mathbf{u}, \quad \nabla \cdot \mathbf{u} = 0, \quad (1)$$

where we have defined the Reynolds number for this flow as $\text{Re}=\rho h U_{\text{ref}}/\mu$. We assume in this paper that the flow satisfies slip boundary conditions on both surfaces, with slip lengths λ_1 and λ_2 at $y^*=h$ and $y^*=-h$, respectively. If we define the Knudsen numbers $\text{Kn}_1=\lambda_1/h$ and $\text{Kn}_2=\lambda_2/h$, and denote by (u, v, w) the streamwise, wall normal, and spanwise components of \mathbf{u} , the boundary conditions for Eq. (1) are $v=0$ at $y=\pm 1$ and

$$u + \text{Kn}_1 \frac{\partial u}{\partial y} = w + \text{Kn}_1 \frac{\partial w}{\partial y} = 0, \quad y = 1, \quad (2a)$$

^{a)}Present address: Department of Mechanical Engineering, Massachusetts Institute of Technology, 77 Massachusetts Ave., Cambridge, MA 02139. Electronic mail: lauga@mit.edu

^{b)}Electronic mail: carlo.cossu@ladhyx.polytechnique.fr

$$u - \text{Kn}_2 \frac{\partial u}{\partial y} = w - \text{Kn}_2 \frac{\partial w}{\partial y} = 0, \quad y = -1. \quad (2b)$$

We are interested in the stability of the steady unidirectional base flow $\mathbf{U} = U(y)\mathbf{e}_x$ satisfying Eqs. (1) and (2),

$$U(y) = 1 + \frac{2(\text{Kn}_1 + \text{Kn}_2 + 2\text{Kn}_1\text{Kn}_2)}{2 + \text{Kn}_1 + \text{Kn}_2} + \left[\frac{2(\text{Kn}_1 - \text{Kn}_2)}{2 + \text{Kn}_1 + \text{Kn}_2} \right] y - y^2. \quad (3)$$

In the absence of slip, $\text{Kn}_1 = \text{Kn}_2 = 0$ and Eq. (3) is reduced to the standard Poiseuille solution, $U(y) = 1 - y^2$. In order to characterize the stability of Eq. (3), we write the total velocity field as the sum of the base flow plus small perturbations, $\mathbf{u} = \mathbf{U} + \mathbf{u}'$ and $p = P + p'$, and linearize the Navier-Stokes equations around (\mathbf{U}, P) . This procedure is classic and we refer, e.g., to Refs. 14 and 16 for the details. The same standard procedure is applied to the boundary conditions [Eq. (2)]. These linear boundary conditions are satisfied by both the total flow $\{u = U + u', v = v', w = w'\}$ and the base flow itself $\{U, 0, 0\}$. Consequently, a simple subtraction shows that the boundary conditions for the perturbations are also of the form of Eq. (2). These boundary conditions are the same as those used by Gersting in his stability analysis¹² and differ from the incorrect boundary conditions used in Refs. 9–11 that implicitly assume $\mathbf{u}' = 0$ at $y = \pm 1$. Therefore, in Refs. 9–11, slip boundary conditions are assumed for the basic flow, but no-slip boundary conditions are used for the perturbations, leading to incorrect results.

Following a standard procedure (see, e.g., Ref. 14 for details), the linearized Navier-Stokes equations are recast in a set of two differential equations for the wall-normal velocity v' and the wall-normal vorticity $\eta' = \partial u' / \partial z - \partial w' / \partial x$. Exploiting the homogeneous nature of the streamwise and spanwise directions, perturbations are Fourier transformed in the form

$$\mathbf{u}'(x, y, z, t) = \hat{\mathbf{u}}(\alpha, y, \beta, t) e^{i(\alpha x + \beta z)}, \quad (4)$$

and therefore $\eta'(x, y, z, t) = \hat{\eta}(\alpha, y, \beta, t) e^{i(\alpha x + \beta z)}$, with $\hat{\eta} = i\beta \hat{u} - i\alpha \hat{w}$. The standard evolution equation for $(\hat{v}, \hat{\eta})$ is finally obtained to be¹⁴

$$\frac{\partial}{\partial t} \begin{pmatrix} \Delta \hat{v} \\ \hat{\eta} \end{pmatrix} = \begin{pmatrix} \mathcal{L} & 0 \\ \mathcal{C} & \mathcal{S} \end{pmatrix} \cdot \begin{pmatrix} \hat{v} \\ \hat{\eta} \end{pmatrix}, \quad (5)$$

where the operators are defined as

$$\mathcal{L} \triangleq -i\alpha U \Delta + i\alpha D^2 U + \Delta(\Delta/\text{Re}), \quad (6)$$

$$\mathcal{C} \triangleq -i\beta D U, \quad (7)$$

$$\mathcal{S} \triangleq -i\alpha U + \Delta/\text{Re}, \quad (8)$$

with $\Delta \triangleq D^2 - \alpha^2 - \beta^2$ and where D denotes derivatives with respect to y . The fourth-order system of equations [Eq. (5)] requires boundary conditions for both \hat{v} and $\hat{\eta}$. Using the continuity equation, $i\alpha \hat{u} + D\hat{v} + i\beta \hat{w} = 0$, together with the boundary conditions in Eq. (2), it is straightforward to show that the boundary conditions for $(\hat{v}, \hat{\eta})$ are

$$\hat{v} = D\hat{v} + \text{Kn}_1 D^2 \hat{v} = 0, \quad y = 1, \quad (9a)$$

$$\hat{v} = D\hat{v} - \text{Kn}_2 D^2 \hat{v} = 0, \quad y = -1, \quad (9b)$$

$$\hat{\eta} + \text{Kn}_1 D \hat{\eta} = 0, \quad y = 1, \quad (9c)$$

$$\hat{\eta} - \text{Kn}_2 D \hat{\eta} = 0, \quad y = -1, \quad (9d)$$

and for simplicity, we restrict the analysis in this Brief Communication to symmetric slip ($\text{Kn}_1 = \text{Kn}_2 = \text{Kn}$) and asymmetric slip cases ($\text{Kn}_1 = \text{Kn}$, $\text{Kn}_2 = 0$). We emphasize again that these boundary conditions are different from those used in Refs. 9–11, where, instead, Kn_1 and Kn_2 were set to zero in Eq. (9).

A Chebyshev collocation method is used to discretize the system [Eq. (5)], and standard methods (described in Ref. 14 and references therein) are then employed to compute eigenvalues, eigenmodes, and maximum transient energy growth. The standard implementation of these methods is modified by changing the standard homogeneous no-slip boundary conditions into the more general slip boundary conditions [Eq. (9)]. All the results presented below have been obtained with 97 collocation points. Convergence of the results has been verified, and the code has been thoroughly tested by comparing both the modal and the nonmodal results in the case of no-slip boundary conditions,¹⁴ as well as with the modal symmetric slip results reported in Ref. 12.

The modal stability analysis assumes solutions in the form of normal modes, $\{\hat{v}, \hat{\eta}\}(\alpha, y, \beta, t) = \{\bar{v}, \bar{\eta}\}(\alpha, y, \beta, \omega) e^{-i\omega t}$, where the complex frequency ω is the solution to an eigenvalue problem [Eq. (5)], which is solved numerically. The flow is found to be linearly unstable if there exists at least one eigenvalue with a positive imaginary part, $\omega_i > 0$. The Squire theorem¹⁶ applies to this flow, and the critical modes are two dimensional (i.e., with $\beta = 0$). The neutral curve $\omega_i(\alpha, \beta = 0, \text{Re}) = 0$ in the symmetric slip case is displayed in Fig. 1(a). The boundary slip is found to significantly shift the neutral curve towards larger values of the Reynolds number, indicating a strongly stabilizing influence of slip on linear stability. Results for the asymmetric slip case, displayed in Fig. 1(b), are similar although less pronounced. The dependence of the critical Reynolds number for linear stability, Re_c , with the Knudsen number Kn is displayed in Fig. 2 and confirms the stabilizing effect of the slip on shear-flow instabilities. Our results, which use the correct boundary conditions [Eq. (9)] agree with the symmetric slip calculations of Ref. 12 but, as expected, are in strong contradiction with the conclusions reported in Refs. 9–11.

In the absence of slip at the walls, the Poiseuille flow is known to undergo a transition to turbulence at Reynolds numbers well below the critical Reynolds number corresponding to the onset of linear modal instability. This subcritical transition scenario has been related to the strongly non-normal nature of the linearized operator [Eq. (5)], explaining the potential of the flow to sustain large transient energy growth, possibly triggering the transition to turbulence for values of the Reynolds number much smaller than Re_c .^{13,14} The standard modal stability analysis is therefore extended to the nonmodal (or generalized¹⁷) stability analy-

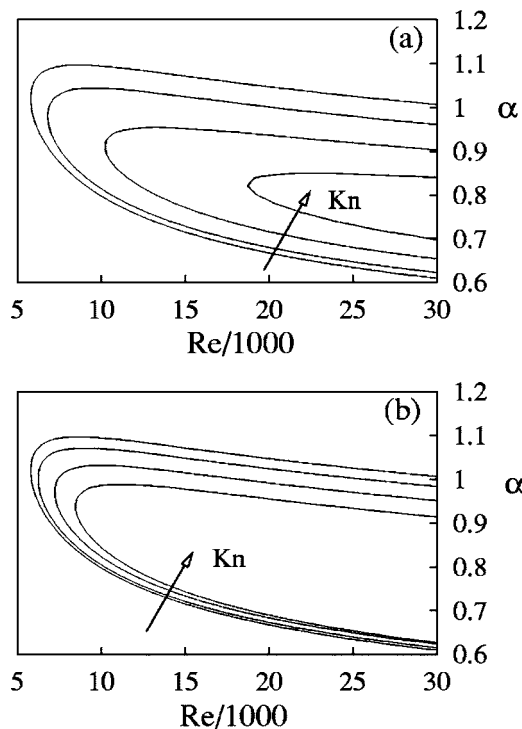


FIG. 1. Neutral curve $\omega_i(\alpha, \beta=0, Re)=0$ for the symmetric slip case (a) and asymmetric slip case (b) and values of $Kn=0$ (no-slip), 0.01, 0.02, and 0.03.

sis where, for instance, the maximum transient energy growth is computed. Let us define, for a given Fourier mode, the instantaneous kinetic energy of the flow perturbations as

$$E(t, \alpha, \beta, \hat{\mathbf{u}}_0) \triangleq \int_{-1}^1 |\hat{\mathbf{u}}(\alpha, y, \beta, t)|^2 dy, \quad (10)$$

which is a function of time and the initial condition, $\hat{\mathbf{u}}_0 \triangleq \hat{\mathbf{u}}(\alpha, y, \beta, 0)$. If we denote by $G(t)$ the energy growth at time t , maximized over all nonzero initial conditions,

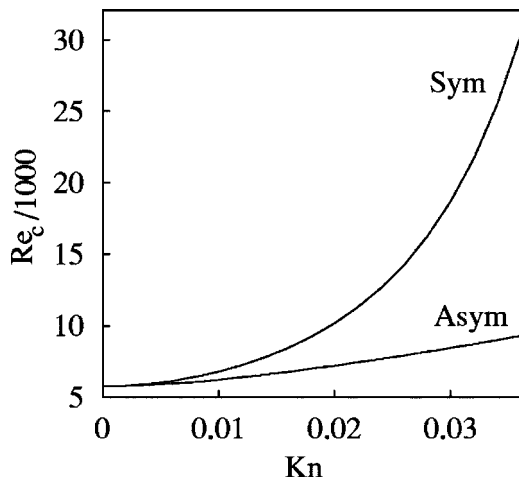


FIG. 2. Critical Reynolds number for linear stability $Re_c(Kn)$ for the symmetric and asymmetric slip cases. In the case of no-slip ($Kn=0$), the critical Reynolds number is 5772.

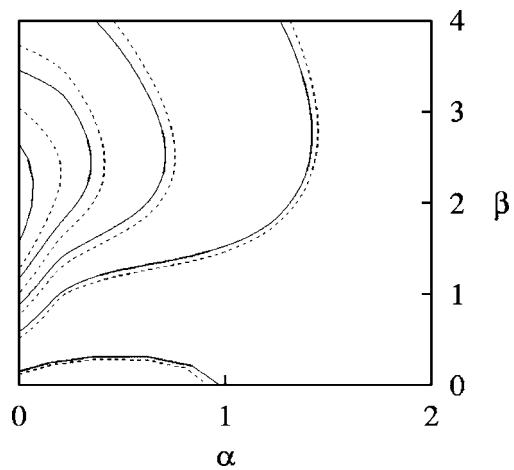


FIG. 3. Map of the isovalues of the maximum transient energy growth $G_{\max}(\alpha, \beta)$ for $Re=1500$ in two cases: No-slip (solid line) and symmetric slip boundary conditions with $Kn=0.03$ (dashed line). The values of G_{\max} are 10, 100, 200, 300, and 400 from the outer to the inner curve.

$$G(t, \alpha, \beta) = \max_{\hat{\mathbf{u}}_0 \neq 0} \left[\frac{E(t, \alpha, \beta, \hat{\mathbf{u}}_0)}{E(0, \alpha, \beta, \hat{\mathbf{u}}_0)} \right], \quad (11)$$

then the maximum transient energy growth possible over all times, $G_{\max}(\alpha, \beta)$, is defined as

$$G_{\max}(\alpha, \beta) = \max_{t \geq 0} G(t, \alpha, \beta). \quad (12)$$

In Fig. 3 we report the isovalues of $G_{\max}(\alpha, \beta)$ computed for $Re=1500$ for both the no-slip (solid line) and the symmetric slip cases (dashed line). Although the maximum energy growth with slip is always larger than in the case of no-slip, the increase is small and therefore slip hardly affects the transient energy growth. The optimal maximum transient energy growth (largest value over all wavenumbers) is obtained for $\alpha=0$ and $\beta=2$ for both slip and no-slip boundary conditions. Figure 4 displays the maximum energy growth as a function of time, $G(t, \alpha=0, \beta=2)$, at $Re=1500$ and in the symmetric slip case for different values of the Knudsen number. The small increase of the optimal growth with Kn appears in all cases. Furthermore, the time where the maximum growth is attained is also slightly increased by the slip. As both the square root of the maximum growth and the time at which it is attained depend linearly on the Reynolds num-

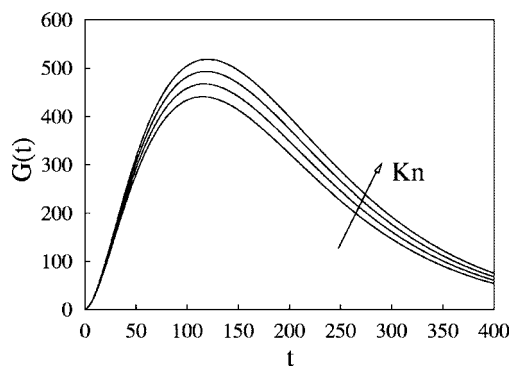


FIG. 4. Maximum energy growth $G(t, \alpha=0, \beta=2)$ at $Re=1500$ and in the symmetric slip case with $Kn=0$ (no-slip), 0.01, 0.02, and 0.03.

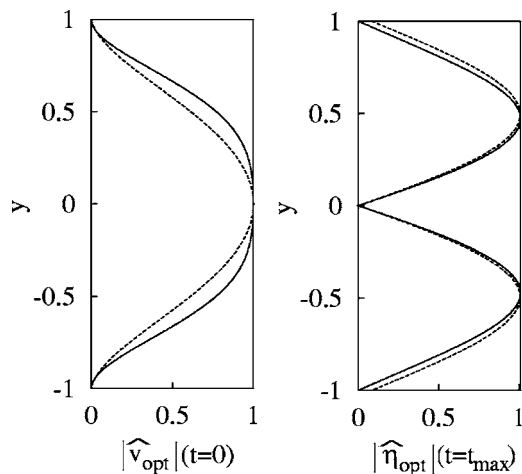


FIG. 5. Optimal initial condition $\hat{v}_{\text{opt}}(t=0)$ and optimal response $\hat{\eta}_{\text{opt}}(t=t_{\text{max}})$ leading to largest transient energy growth at $\text{Re}=1500$ and for $(\alpha, \beta)=(0, 2)$, for both no-slip (solid line) and symmetric slip (dashed line) cases with $\text{Kn}=0.03$.

bers, these effects suggest that the effect of slip induces an increase of an effective Reynolds number, which is consistent with the observation that slip flows have, for the same pressure forcing, a larger flow rate than do no-slip flows.

In the case of no-slip channel flows it is known that the initial perturbations inducing the largest energy growth are streamwise vortices, while the most amplified response consists of streamwise streaks. Translated in terms of the v' and η' variables, this means that the optimal initial perturbations are v type, with η negligible, while, on the contrary, the most amplified response is η type, with v negligible. This is also the case with slip boundary conditions. In Fig. 5 we reproduce, for $\text{Re}=1500$, the optimal initial condition $\hat{v}_{\text{opt}}(y, t=0)$ (left) and the optimal response $\hat{\eta}_{\text{opt}}(y, t=t_{\text{max}})$ (right) corresponding to the largest transient energy growth $G_{\text{max}}(\alpha=0, \beta=2)$. The shape of the optimal initial perturbation differ slightly from the no-slip case, while the optimal responses are nearly undistinguishable, except near the wall, where the effect of the slip boundary conditions is apparent.

The lift-up mechanism, by which low-amplitude vortices are converted into large amplitude streaks, seems therefore to be only slightly sensitive to slip boundary conditions at the wall. Similar results are obtained for other values of Kn and Re and for asymmetric slip boundary conditions.

We thank Howard Stone for the useful feedback. E.L. gratefully acknowledges the funding by the Office of Naval Research (Grant No. N00014-03-1-0376) and the Harvard MRSEC.

¹C. M. Ho and Y. C. Tai, "Micro-electro-mechanical-systems (MEMS) and fluid flows," *Annu. Rev. Fluid Mech.* **30**, 579 (1998).

²H. A. Stone, A. D. Stroock, and A. Ajdari, "Engineering flows in small devices: Microfluidics toward a lab-on-a-chip," *Annu. Rev. Fluid Mech.* **36**, 381 (2004).

³T. M. Squires and S. R. Quake, "Microfluidics: Fluid physics at the nanoliter scale," *Rev. Mod. Phys.* **77** (in press).

⁴S. Goldstein, *Modern Development in Fluid Dynamics* (Clarendon, Oxford, 1938), Vol. 2, pp. 676–680.

⁵O. I. Vinogradova, "Slippage of water over hydrophobic surfaces," *Int. J. Min. Process.* **56**, 31 (1999).

⁶S. Granick, Y. X. Zhu, and H. Lee, "Slippery questions about complex fluids flowing past solids," *Nat. Mater.* **2**, 221 (2003).

⁷P. Tabeling, "Slip phenomena at liquid-solid interfaces," *C. R. Phys.* **5**, 531 (2004).

⁸E. Lauga, M. P. Brenner, and H. A. Stone, in *Handbook of Experimental Fluid Dynamics*, edited by J. F. Foss, C. Tropea, and A. Yarin (Springer, New York, in press).

⁹A. K. H. Chu, "Stability of incompressible helium II: A two-fluid system," *J. Phys.: Condens. Matter* **12**, 8065 (2000).

¹⁰A. K. H. Chu, "Stability of slip flows in a peristaltic transport," *Europhys. Lett.* **64**, 435 (2003).

¹¹A. K. H. Chu, "Instability of Navier slip flow of liquids," *C. R. Mec.* **332**, 895 (2004).

¹²J. M. Gersting, "Hydrodynamic stability of plane porous slip flow," *Phys. Fluids* **17**, 2126 (1974).

¹³L. N. Trefethen, A. E. Trefethen, S. C. Reddy, and T. A. Driscoll, "Hydrodynamic stability without eigenvalues," *Science* **261**, 578 (1993).

¹⁴P. J. Schmid and D. S. Henningson, *Stability and Transition in Shear Flows* (Springer, New York, 2001).

¹⁵K. M. Butler and B. F. Farrell, "Three-dimensional optimal perturbations in viscous shear flow," *Phys. Fluids A* **4**, 1637 (1992).

¹⁶P. G. Drazin and W. H. Reid, *Hydrodynamic Stability* (Cambridge University Press, Cambridge, UK, 1981).

¹⁷B. F. Farrell and P. J. Ioannou, "Generalized stability theory. I. Autonomous operators," *J. Atmos. Sci.* **53**, 2025 (1996).